


Review

Recent Progress in Nitrogen-Doped Metal-Free Electrocatalysts for Oxygen Reduction Reaction

Zexing Wu ^{1,*}, Min Song ¹, Jie Wang ^{2,*} and Xien Liu ^{1,*} 

¹ Key Laboratory of Sensor Analysis of Tumor Marker of Education Ministry, State Key Laboratory Base of Eco-chemical Engineering, College of Chemistry and Molecular Engineering, Qingdao University of Science & Technology, 53 Zhengzhou Road, Qingdao 266042, China; songm1126@163.com

² Department of Applied Physics, The Hong Kong Polytechnic University, Hung Horn, Kowloon 999077, Hong Kong, China

* Correspondence: splswzx@qust.edu.cn (Z.W.); jw65111@gmail.com (J.W.); liuxien@qust.edu.cn (X.L.); Tel.: +86-0532-8402-3409 (Z.W.)

Received: 16 April 2018; Accepted: 2 May 2018; Published: 7 May 2018



Abstract: Electrocatalysis for the oxygen reduction reaction (ORR) at the cathode plays a critical role in fuel cells and metal-air batteries. However, the high-cost and sluggish kinetics of the catalytic reaction have hindered its development. Therefore, developing efficient catalysts to address these issues is of vital significance. In this work, we summarized the recent progress of nitrogen (N)-doped metal-free catalysts for the ORR, owing to their high catalytic activity (comparable to Pt/C) and cost-effectiveness. The synthetic strategy and the morphology structure to catalytic performance are mainly discussed. Furthermore, the design of N-doped nanomaterials with other heteroatoms in aiming to further enhance the ORR performance is also reviewed. At the end of the review, we provide a brief summary of the N-doped carbon-based catalysts in enhancing the ORR performance and give future perspectives for their further development.

Keywords: nitrogen-doped carbon; metal-free; electrocatalysis; oxygen reduction reaction; perspectives

1. Introduction

Increasingly severe environmental problems have created the need to develop renewable energy conversion and storage devices. Among the various new energy systems, fuel cells and metal air batteries are known as two of the best substitutes for traditional fossil fuels, due to their high theoretical capacity and energy density. For a fuel cell or metal air battery, the oxygen reduction reaction (ORR) at the cathode is an essential and significant electrochemical reaction which is also recognized as the “short board” in the battery, because the sluggish kinetics of the ORR restricts the efficiency and performance of such devices [1–7]. On the other hand, at present, Pt-based electrocatalysts are well known to exhibit the best ORR performance in both acid and alkaline media [8,9]. However, the high cost and scarcity of these metals cannot be ignored when considering the scalable applications of fuel cells and metal-air batteries [10,11]. Thus, research focused on non-precious metals or metal-free catalysts with low-cost, high performance, and excellent durability to replace Pt-based catalysts for the ORR has attracted tremendous attention [12,13]. Among the non-precious electrocatalysts, heteroatom-doped carbon materials as metal-free catalyst have been extensively investigated [14–16], due to their abundant reserves, excellent catalytic activity, high electron conductivity, and environmental friendly characteristics.

Various heteroatoms, such as N [17], S [18], P [19], B [20], and I [21], have been introduced into pure carbon materials in order to enhance the conductivity and tune the electron distribution which

improve the ORR reaction kinetics. It should be noted that nitrogen-doped carbon nanomaterials are the most commonly investigated for the ORR relative to other heteroatoms. This can be explained by the obvious electronegativity difference between C ($\chi = 2.55$) and N ($\chi = 3.06$), which polarizes the carbon matrix efficiently and facilitates the adsorption of oxygen. Besides, the resource of nitrogen is more abundant and environmentally friendly than other heteroatoms. Doping with N changes the charge redistribution and then enhances the ORR activity. At the electrode interface, the chemisorption of O_2 on the catalyst would be changed from the usual end-on adsorption (Pauling model) to a side-on adsorption (Yeager model) which can effectively weaken the O–O bond and is thus more conducive to the process of the ORR [22]. It should be noted that the catalytic performance of N-doped carbon nanomaterials is also correlated with the type of N in the electrocatalysts [23]. In general, the type of N in the carbon frameworks can be divided into three forms: graphitic N (400.9 eV), pyrrolic N (398.6 eV), and pyridinic N (397.9 eV) [24]. Pyridinic N possesses a lone electron pair which is deemed as the active site to enhance the electron donating capability and effectively weaken the O–O band [25,26]. Besides, some researchers considered graphitic N for the active sites due to the coexistence of different kinds of N [27,28]. Guo et al. recently demonstrated that the active sites in N-doped carbon nanomaterials are located at the carbon atoms with Lewis basicity adjacent to pyridinic N [23]. As well as the types of N, the content of N in the electrocatalyst is also a controversial factor affecting the ORR performance, where catalysts with excessive N have inferior ORR activity [29]. According to recent reports, a variety of N-doped carbon nanomaterials have been investigated as metal-free catalysts for the ORR, including carbon nanosheet [30], carbon nanotube [31], graphene [32–34], and composites of carbon nanotube/graphene [35–37]. The carbon materials with different structures show different catalytic activities after doping with N [38]. Thus, the carbon nanomaterial morphology is another used factor to control the catalytic performance, especially the activity and long-term stability.

Although N-doped metal-free catalysts have yielded tremendous advances for the ORR, the catalytic performance is still fall behind of commercial Pt [39]. Considerable efforts have been devoted to optimizing the catalytic performance of N-doped metal-free nanomaterials. It has been found that the introduction of other heteroatoms, such as P [40], S [39], B [41], and so on [42], to form two or three co-doped heteroatoms carbon nanomaterials can further enhance the catalytic activity. For example, S atoms are of particular interest as they were found to easily replace the C atom when co-doping with N [43,44]. For N and P co-doped catalysts, phosphorous exhibits a larger atomic size but a lower electronegativity relative to C, which can create defects on the carbon surface-induced active sites for oxygen adsorption during the ORR [45]. The improvement of the electrocatalytic activity can be attributed to the synergistic effects between the doped heteroatoms. Besides co-doping, the preparation of catalysts with various structures can also effectively enhance the catalytic performance, such as three-dimensional structure [46,47], aerogel [48], and carbon frameworks [17]. In this review, we mainly focus on the recent progress of N-doped carbon nanomaterials and the strategies to enhance the N-doped metal-free catalysts for the ORR. We begin by reviewing synthetic strategies and then we review recent progress on how to further enhance the ORR performance. The challenges and perspectives in this field are also addressed in the final section.

2. Recent Development of Synthetic Methodologies

The synthesis of N-doped carbon-based nanomaterials is divided into three main categories: (i) synthesis of nanocarbon-based materials and then doping with N via N-contain resources, like urea, NH_3 H_2O or NH_3 [49,50] (Figure 1a), et al. (ii) the N-doped carbon nanomaterials obtained by pyrolysis of biomass materials (e.g., prawn shells [51,52], Nori [53], ginkgo leaves [54], fermented rice [55], et al.). This kind of material is beneficial due to their abundance in nature, which creates the potential for large-scale production. (iii) Direct synthesis of N-doped carbon via N-containing carbon precursors, such as polypyrrole [56] and polyaniline [57], gelatin [58], etc., by a direct incorporation of nitrogen atoms into carbon-based nanomaterials (Figure 1b). Such synthetic methods suffer from the relatively high costs of the N-containing precursors.

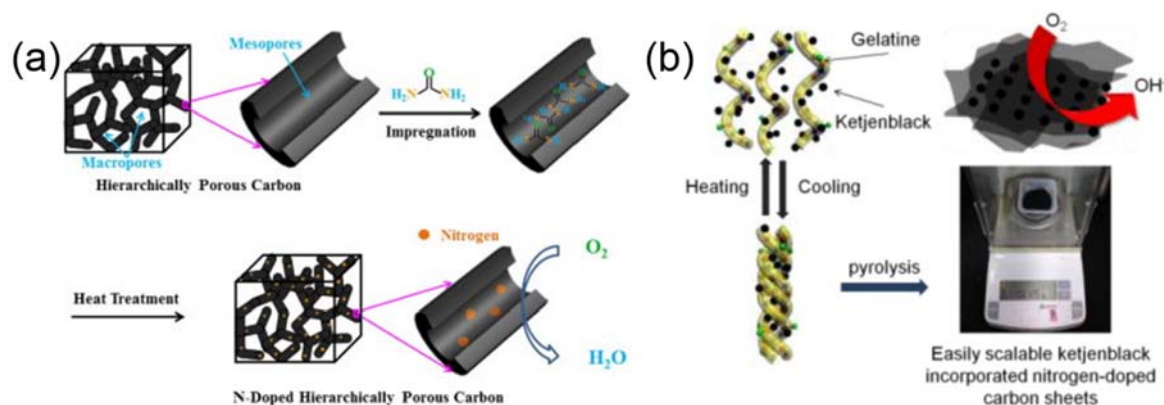


Figure 1. Schematic preparation of N-doped metal-free carbon-based nanocatalysts using urea as N source (a) [50] Copyright 2015 Elsevier and pyrolysis of N-containing precursor (b) [58]. Copyright 2014 American Chemical Society.

Apart from the above synthetic method, to confirm the N was successfully doped into the nanocarbon materials framework, a hydrothermal, solvothermal, or high temperature annealing approach is necessary [48,59,60]. Through these methods, the N-containing small molecules or N-containing carbon materials undergo pyrolysis or carbonization, in which the N would combine with carbon frameworks and then form three kinds of N types: pyridinic N, pyrrolic N, and graphitic N. Besides, the hydrothermal or solvothermal products experienced post-heating annealing are often used to optimize the catalytic activity due to the enhancement of their electronic conductivity for the catalysts and removal of extra impurities. Therefore, detailed discussion of the recent reports on the synthetic methodologies are shown in the following content.

2.1. Co-Pyrolysis of Carbon Materials and N-Containing Sources

Among the various N-containing sources, NH_3 is a widely used nitrogen resource in preparing N-doped carbon-based metal-free electrocatalysts because of its ubiquitous distribution in a tube furnace at high annealing temperatures. Recently, N-doped 3D cross-linking hierarchically porous carbon (LHNHPC) was successfully prepared through a simple two-step process [61] (Figure 2a), in which NH_3 plays an important role in creating pores and defects in the carbon framework. The specific surface area increased with the increasing of temperature, meanwhile, the micropore area decreased which may be due to the disintegration of micropores at high temperature which then evolved into mesopores. Relative to a microporous structure, mesoporous and microporous structures can effectively enhance the catalytic performance of the ORR, while micropores are kinetically inaccessible for O_2 [62]. N-doped hollow mesoporous carbon spheres (NHCSs) were also prepared via a hydrothermal- NH_3 treated strategy (Figure 2b) by using hexamethylenetetramine as the carbon precursor, which also presents excellent catalytic activity for the ORR [63]. Besides NH_3 , urea is a general reactant in preparing N-doped metal-free catalysts due to its moderate pyrolysis temperature (lower than $200\text{ }^\circ\text{C}$), high N content, low cost, and environmental friendly merits. Urea can form graphitic carbon nitride ($\text{g-C}_3\text{N}_4$) at about $550\text{ }^\circ\text{C}$ which can act as a template to form a nanosheet structure [64]. The formed $\text{g-C}_3\text{N}_4$ will be decomposed into NH_3 and carbon nitride gases which can dope into the carbon frameworks [65]. EDTA is another N source which is commonly used act as a complexing agent in chemical science. It also possesses a high N content for doping into the carbon frameworks [12,66].

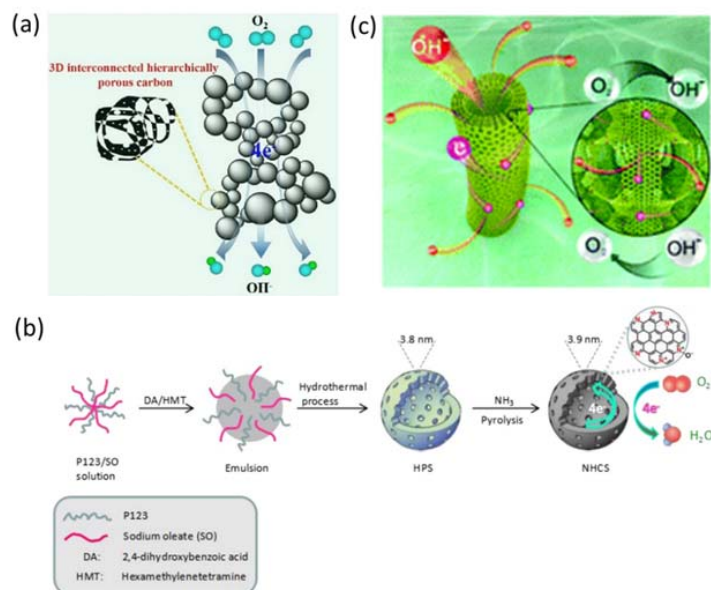


Figure 2. Schematic illustration images of the N-doped carbon-based materials preparation. (a) LHNHPC, [61]. Copyright 2017 Elsevier (b) NCMT, [63]. Copyright 2017 Elsevier and (c) NHCSs, [67]. Copyright 2016, Royal Society of Chemistry.

2.2. Pyrolysis of Biomass Materials

Biomass carbon materials are ubiquitous in earth. They are abundant resources of ultra-low cost and are easy to acquire. Therefore, great efforts have been devoted to improving their catalytic performance towards the ORR. Facial cotton, a kind of makeup tool which features 100% cotton and is naturally derived, has been investigated as a carbon precursor in the synthesis of N-doped porous carbon. Li and co-workers [67] prepared flexible three dimensional (3D) sponges composed of porous N-doped carbon microtubes (NCMTs) by pyrolysis of facial cotton under NH₃ atmosphere (Figure 2c). The obtained NCMTs were characterized by dictyophora morphology with micro-scale hollow cores and interconnected tube walls. They also possess high specific surface area (2358 m² g⁻¹) which endows them with abundant active sites and mass transfer channels. Thus, the synthesized catalysts exhibit excellent bifunctional catalytic performance towards the ORR and OER. Yu and co-workers [68] developed a highly active nitrogen-doped carbon nanofiber (N-CNF) aerogel by direct pyrolysis of the cheap, green, mass-producible biomass of bacterial cellulose, followed by NH₃ activation. When used as a metal-free electrocatalyst, it had superior ORR activity, high selectivity, and excellent electrochemical stability. Chen and co-workers [69] investigated biomass materials from the plant *Typha orientalis*. After high temperature annealing, nitrogen-doped carbon nanosheets with high surface area (898 m² g⁻¹), abundant micropores, and a high content of nitrogen (highest content of 9.1 at.%) were successfully prepared which exhibited a, surprisingly high ORR activity. The use of lignin as a precursor for the preparation of ORR electrocatalysts is an interesting option from a sustainability standpoint. Esposito and co-workers [70] illustrated the preparation of nitrogen-doped carbon (NDC) with micro-, meso-, and macroporous structure by using lignin extracted from beech wood via alkaline hydrothermal treatment and successively functionalized via aromatic nitration. After being carbonized in the eutectic salt melt KCl/ZnCl₂, the NDC exhibited excellent electrocatalytic performance towards the ORR.

2.3. Pyrolysis of N-Containing Carbon Precursors

N-doped carbon metal-free electrocatalyst can also be obtained from the decomposition of nitrogen and carbon-containing precursors [71–73]. At present, metal-organic framework (MOF) has been widely investigated to prepare N-doped carbon nanomaterials for ORR [74,75]. MOF is a novel porous

materials which has some advantages relative to traditional porous materials, including structural diversity, high-surface area, diverse nanostructures, and good designability [76]. Thus, MOF has been applied in gas adsorption and storage [77] and electrocatalyst [78] etc. [79]. Zhang et al. [74] prepared nitrogen-doped porous carbon nanopolyhedra derived from ZIF-8 which possess excellent electrocatalytic activity for ORR in 0.1 M KOH (Figure 3a). The obtained nanomaterials present some attracting features, including a high degree of graphitization and high specific surface area with hierarchical porous structure, which are beneficial for catalytic processes. The catalytic activity for the ORR correlates to the types of N in the catalyst and the degree of the graphitization. Li et al. [80] synthesized electrocatalysts for the ORR with a high degree of graphitization and pyridinic-N dopants by pyrolysis pyridyl-ligand-based MOF (Figure 3b). The prepared MOF exhibits a rod-like structure and foam morphology nanomaterials were formed, composed of curved graphene nanosheets after carbonization. It was found that the graphitization degree increased as the pyrolysis temperature increased, but the content of pyridinic-N content decreased, which can decrease the electron transfer resistance. The obtained nanomaterials possess the best catalytic activity for ORR in alkaline electrolyte at high temperatures, demonstrating that the graphitization degree of the electrocatalyst affects the catalytic performance. Most sizes of MOF are too large even after carbonization to provide abundant active sites for electrocatalytic processes to occur. Jiang et al. [81] developed a facile strategy using cetyltrimethylammonium bromide (CTAB) micelles to control the size of ZIF-8 (Figure 3c). As a result, the size of PC1000@C from ZIF-8@CTAB is about 40 nm which is much smaller than PC 1000 (290 nm) from ZIF-8, demonstrating CTAB can efficiently manipulate and control the size of ZIF-8. Furthermore, PC 1000@C presents higher specific surface area, pore volume, and a more mesoporous structure relative to PC 1000, from which we can deduce that the addition of CTAB affects the nanostructure of the catalyst. Wang and co-workers [73] derived well-defined carbon nanotubes with controlled doping of various N species (e.g., pyrrolic, pyridinic, and graphitic N) have been achieved by in situ pyrolysis of polyaniline (PANI) nanotubes at different temperatures. As a result, carbon nanotubes fabricated at 700 °C exhibited the highest electrocatalytic ORR activity, long-standing stability, and good tolerance against methanol in alkaline medium, which is mainly attributed to the high nitrogen level of the active pyridinic and graphitic N.

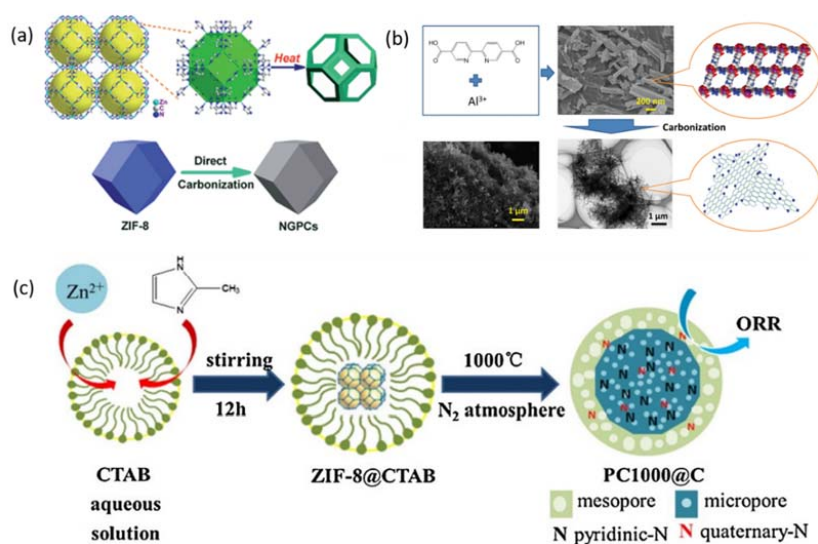


Figure 3. (a) Schematic illustration of the nanoscale MOF (NMOFs)-driven template synthesis of highly graphitized nitrogen-doped porous carbon nanopolyhedra [74]; Copyright 2014, Royal Society of Chemistry (b) the synthesis process of PNPC-1000 and corresponding SEM and TEM images [80]; Copyright 2016, Royal Society of Chemistry (c) schematic illustration of PC1000@C derived from ZIF-8@CTAB [81]. Copyright 2016, Elsevier.

3. Further Strategies to Enhance the ORR Performance

Although N-doped carbon nanomaterials have achieved great progress towards efficient ORR, the catalytic performance still does not meet the practical need. Therefore, it is urgent to develop other strategies to further enhance the catalytic performance.

3.1. Coordination with Other Heteroatoms

As mentioned in the introduction part, the coordination with other heteroatoms to enhance the ORR performance is an important strategy to optimize the electrocatalytic activity of N-doped nanomaterials. It should be noted that the S atom is of particular interest because it was found to easily replace the C atom when co-doping with N [43,44]. Qu and co-workers [82] prepared N,S co-doped carbon nanosheets (N,S-CN) by using sulfur-modified GO-PDA (polydopamine) as the substrate, where PDA and 2-mercaptoethanol served as the N and S sources, respectively (Figure 4a). As a result, N,S-CN presents the best catalytic activity with a high onset potential and half-wave potential relative to solely N-doped carbon nanosheets (N-CN). Besides, this catalyst also exhibited the lowest Tafel slopes relative to other two catalysts, close to Pt/C, demonstrating the favorable ORR kinetics of the co-doped nanomaterials. Honeysuckles are arching shrubs or twining vines in the family Caprifoliaceae, native to the Northern Hemisphere. Gao and co-workers [36] prepared a three-dimensional (3D) porous sulfur, nitrogen co-doped carbon using honeysuckle as the single precursor. Such excellent ORR performance may be ascribed to the synergistic effects of the numerous ORR catalytic sites provided by sulfur–nitrogen hetero-doping, favorable reactant transport channels provided by pore structures, and fast electron transfer rate induced by 3D continuous networks. Thus, the addition of S to the N-doped nanomaterials were proven to be an efficient strategy to enhance the catalytic activity. Besides S, phosphorous (P) is the other general atom to exhibit an coordination effect towards ORR when coupled with N [83,84]. Jiang and co-workers [85] reported an N and P co-doped electrocatalyst prepared via a self-assembly strategy by using melamine and ATMP as the gelator. As shown in Figure 4d, the CV curves measured in N₂ and O₂ saturated 0.1 M KOH demonstrate that the coexistence of N and P (NPCN) can enhance the catalytic activity relative to solely N or P doped nanomaterials, consistent with the LSVs in Figure 4d. The excellent catalytic activity of NPCN-900 can be attributed to the synergistic effect between N and P. The N dopants can change the electric neutrality of the carbon atoms and then P dopants can enlarge the spin density, resulting in unevenly distributed charge density [86]. Furthermore, the addition of P in the carbon nanomaterials can introduce defects and edges which can serve active sites for the ORR. Thus, the addition of other heteroatoms can effectively enhance the catalytic activity for the ORR.

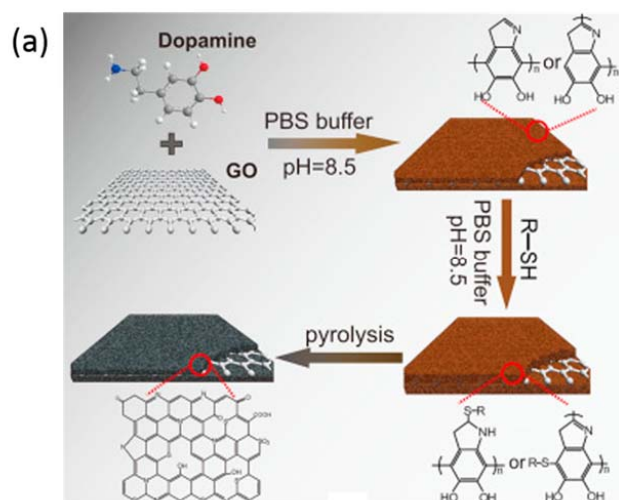


Figure 4. Cont.

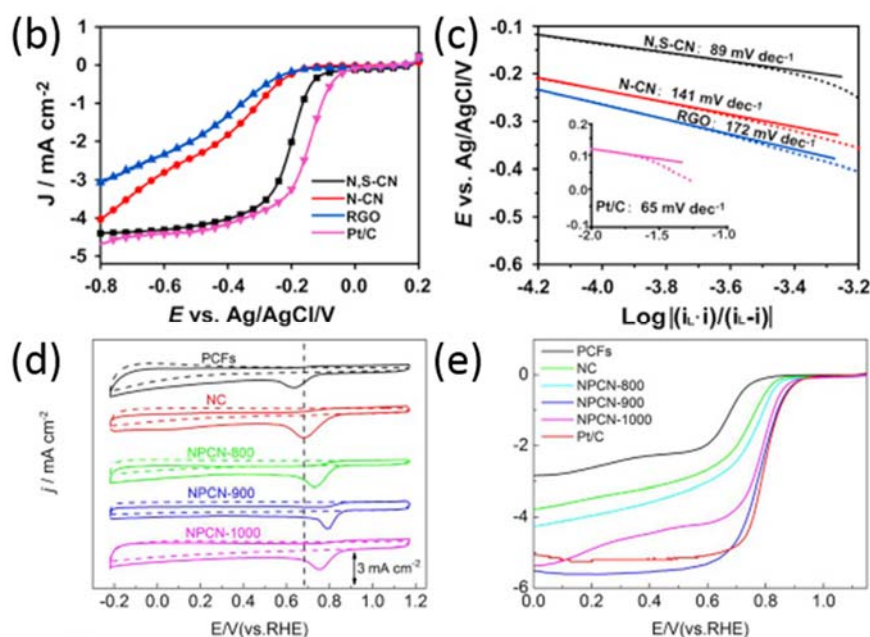


Figure 4. (a) Schematic illustration of the preparation of N,S-CN. ORR LSVs (b) and Tafel slope (c) of N,S-CN, N-CN, RGO, and Pt/C [82]. Copyright 2016 Elsevier. CV curves in N₂ and O₂-saturated 0.1 M KOH (d) and LSVs curves of PCFs, NC, NPCN-900, NPCN-900, and NPCN-1000 (e) [85]. Copyright 2017 Elsevier.

3.2. Structure Modification

The structure and morphology of the catalyst materials play a significant role in ORR performance. Among the various catalyst materials, graphene is a popular two-dimensional (2D) nanomaterials for ORR due to its outstanding properties, especially its high surface area (2630 m² g⁻¹), which provides a high density of active sites [87]. Furthermore, this material possesses excellent electrical conductivity [88], mechanical strength, and stability [89]. Thus, graphene and graphene-like 2D nanomaterials have been widely studied for ORR [90]. Besides graphene, graphitic carbon nitride (g-C₃N₄) is a quasi-2D organic nonmetallic semiconductor [91] which has been widely used as a template to prepare 2D carbon nanomaterials [92]. Yu et al. [93] prepared N-doped carbon nanosheets (N-CNS), using g-C₃N₄ as the template and nitrogen source. The N-CNS features a high specific surface area and a porous structure which exhibits superior ORR performance (Figure 5a). The porous structure in the catalyst benefits the mass transport during the catalytic process and combining 2D nanomaterials with porous structure leads to outstanding ORR catalytic performance. Wei and co-workers [30] prepared N-doped carbon nanosheets (NDCN) with uniform mesopores using silica as the template and PDA as the N and C source. The size of the mesopores can be tuned in the preparation of this materials (Figure 5b). The electrocatalytic activity of the nanomaterial is closely related to the pore size, and the NDCN with pore size of about 22 nm (NDCN-22) exhibited the best catalytic activity. The prepared nanomaterials had typical 2D morphology, uniform and size-defined mesopores, and the mesopores were interconnected on the surface to form 2D planar mesoporous shells (Figure 5c,d).

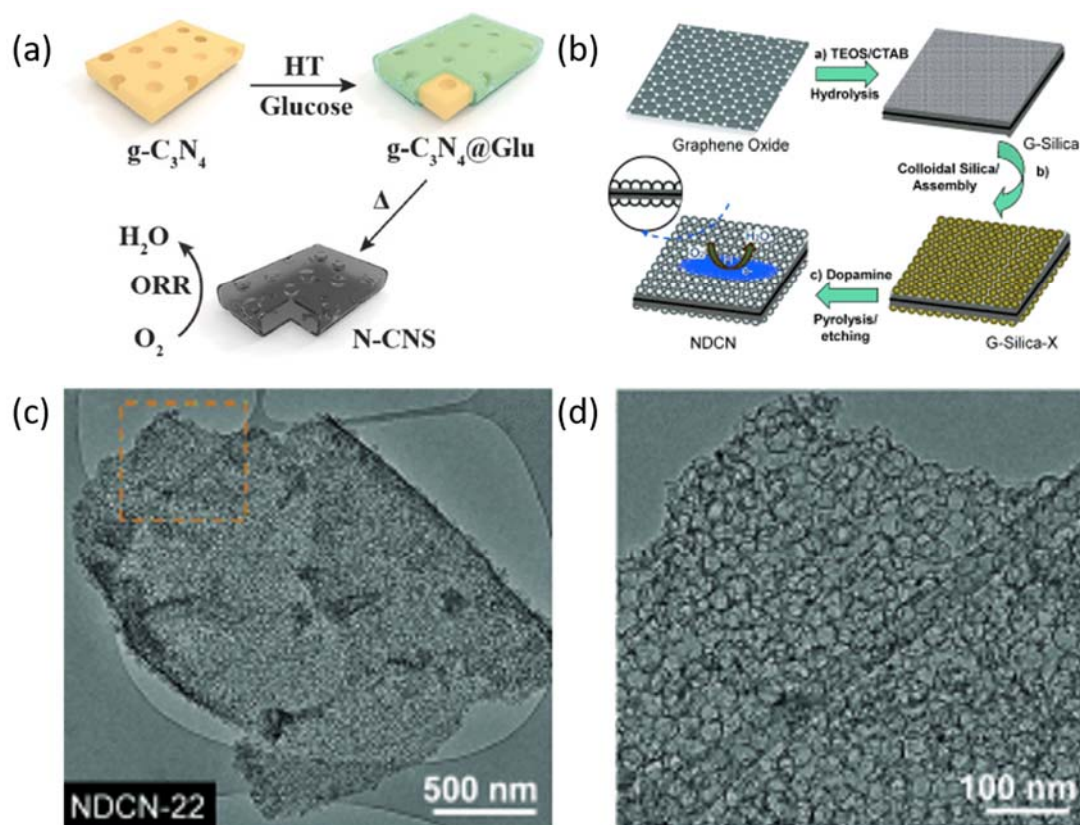


Figure 5. (a) Schematic for the synthesis of N-CNS [93]. Copyright 2016, Wiley-VCH. Copyright 2014, Wiley-VCH. Synthesis of NDCN-x (b) and corresponding TEM images of NDCN-22 (c,d) [30]. Copyright 2014, Wiley-VCH.

Besides 2D nanomaterials, three-dimensional (3D) structured materials are another kind of interesting nanomaterials for ORR, especially those with hollow structures, which can provide ultra-high specific area and an abundance of pores on the spherical walls that provide a triple phase region to benefit the mass transfer of oxygen and electrolytes during the ORR process [94,95]. Wang's group have extensively investigated 3D nanomaterials for ORR [93,96–99]. For metal-free electrocatalysts, N,S-hcs nanomaterials with 3D hollow structures doped with N and S were prepared through a soft template approach (Figure 6a) [96]. The obtained catalyst exhibited high surface area and a mesoporous structure, which provided abundant active sites and rapid mass transfer rate. As a result, the N,S-hcs nanomaterials exhibit excellent catalytic activity, including highly positive onset and half-wave potential. Graphene, a typical 2D nanomaterial, has been widely investigated for ORR, but the severe aggregation due to the π interaction during the thermal annealing process and electrochemical measurement lowers its surface area and mass transfer rate [100,101]. Thus, a new strategy is urgently needed to settle this issue. Wang and co-workers [99] partially exfoliated multi-walled carbon nanotubes (MWCNT) to obtain nanomaterials with the coexistence of graphene and MWCNT which feature a 3D nanostructure and efficiently avoid the aggregation of graphene. The authors used different masses of KMnO_4 as “scissors” to exfoliate MWCNT. The mass ratio 1:3 (MWCNT: KMnO_4) showed the best catalytic activity for ORR (Figure 6b) and it exhibited the closest Tafel slope to Pt/C (Figure 6c). Meanwhile, the prepared NSCNT-3 exhibited a 4-electron reaction pathway obtained through the Koutecky–Levich formula (Figure 6d) and rotating ring disk electrode (RRDE) (Figure 6e) which is in accordance with Pt/C. Wu et al. [95] inserted carbon black into graphene to avoid the aggregation of graphene and the obtained nanomaterials exhibited high specific surface area and attractive catalytic performance.

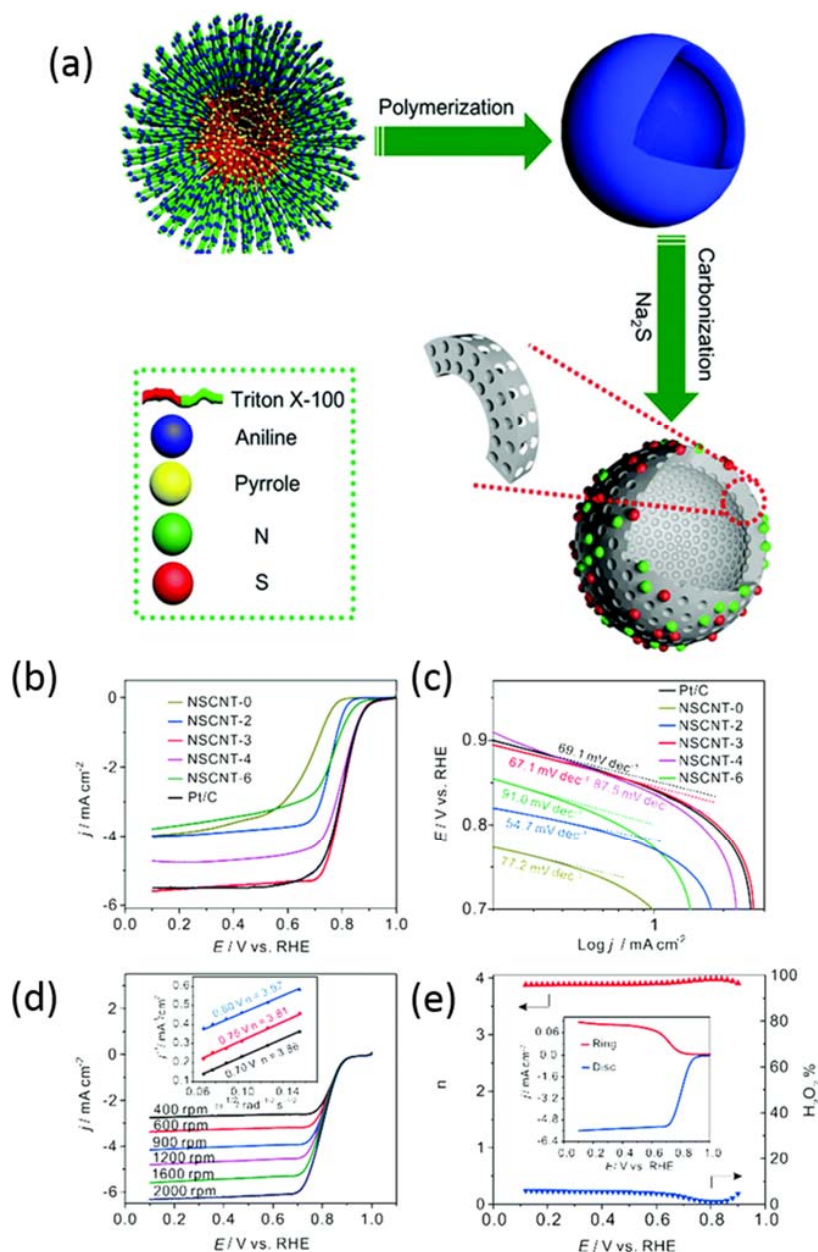


Figure 6. (a) Schematic illustration of the synthesis of N,S-hcs [96]. Copyright 2016, Royal Society of Chemistry. LSVs of NSCNT and Pt/C (b) and corresponding Tafel slopes (c) in 0.1 M KOH solution. (d) LSVs of NSCNT-3 in different rotating speeds and its corresponding Koutecky–Levich value at different potentials. (e) The electron transfer number *n*, H₂O₂ yield, and RRDE voltammograms of NSCNT-3 [99]. Copyright 2016, Royal Society of Chemistry.

3.3. Introduction of Defects

Defects in the nanomaterials can change the electron-hole symmetry and electronic structure, which would facilitate the catalytic activity towards ORR [102–104]. Wang and co-workers [105] categorized the defects into four kinds, including point defects, line defects, plane defects, and volume defects. The created defects in the carbon can provide abundant edges in the defect site and the edges provide large locations for N incorporation. He and co-workers [106] prepared N-doped carbon nanoribbons (NDCNRs) by using pyrrole and aniline as monomers with different ratios to synthesize the nanofibers, and NH₄F as a reactant to produce defects in the nanomaterials. As a result, the optimum catalytic performance was found at an aniline to pyrrole ratio of 1:3, where a

distinct oxygen reduction peak was present at 0.8 V (Figure 7b,c). The highest double layer capacitance can provide abundant active sites for the ORR. The authors found that F-NDCNRs had the highest disorder degree from Raman analysis, and thus could generate catalytically active sites on carbon nanomaterials [107].

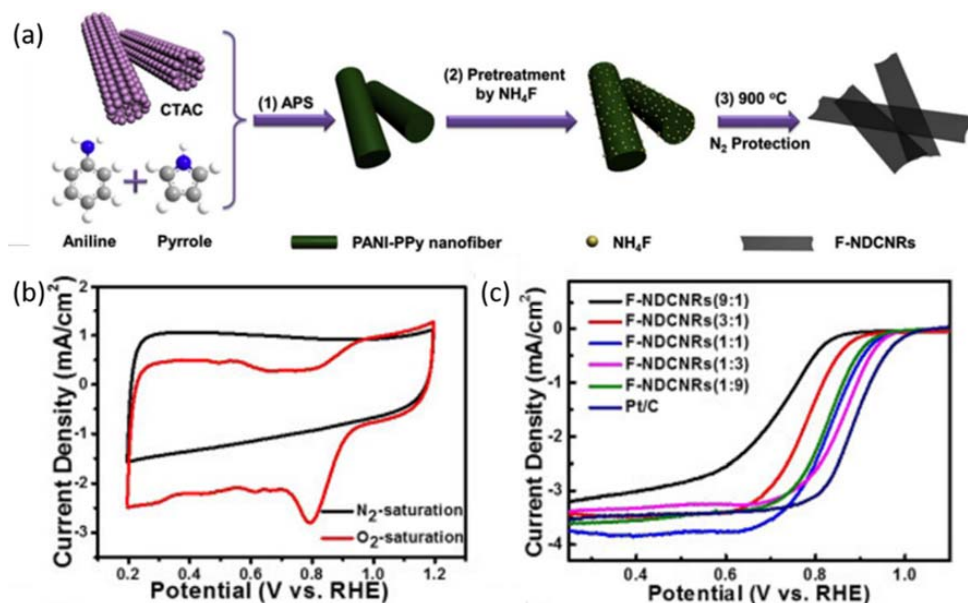


Figure 7. (a) Schematic illustration of preparing F-NDCNRs (x); (b) CV curve of F-NDCNRs (1:3) in N_2 and O_2 -saturated 0.1 M KOH; (c) LSVs of F-NDCNRs (x) with a rotating rate of 900 rpm [106]. Copyright 2017 Elsevier.

Table 1 displays the parameters of the N-doped carbon-based materials which have been applied to the ORR. The parameters include the use of precursors, synthetic methodologies, specific surface area, and half-wave potential. Some conclusions can be drawn from Table 1. (i) The target of lowering the synthetic cost is becoming prevalent; (ii) materials with mesopores are more likely to exhibit superior ORR performance; (iii) the half-wave potential is reaching a bottleneck which will require more efforts to overcome.

Table 1. Parameters of N-doped carbon-based materials applied for ORR.

Materials	Precursor	Methodology	S [$m^2 g^{-1}$]	Half-Wave Potential	Ref.
LHNHPC	Resorcinol, formaldehyde	carbon-aerogel	2600	0.86 V vs. RHE	[61]
NHCSs	hexamethylenetetramine	hydrothermal method	820	-0.215 V vs. SCE	[63]
NCMTs	facial cotton	Pyrolyzing method	2358	/	[67]
N-CNF	bacterial cellulose	Pyrolyzing method	916	0.80 V vs. RHE	[68]
NCS	Typha orientalis	hydrothermal process	898	-0.75 V vs. RHE	[69]
NDC	Nitro Lignin	hydrothermal treatment	1589	0.85 V vs. RHE	[70]
NGPCs	NMOF	carbonization process	932	-0.20 vs. Ag/AgCl	[74]
PNPC	pyridyl-ligand	carbonization	1180	/	[80]
PC1000@C	ZIF-8@CTAB	carbonization	1116	/	[81]
N,S-CN	graphene oxide-polydopamine hybrids	carbonization	273	-0.15 V vs. Ag/AgCl	[82]
PHC	honeysuckles	carbonization	803	/	[36]
NPCN-900	CQDs and ATPM	pyrolysis	743	0.78 V vs. RHE	[85]
NPCNT-2	partially exfoliated MWCNTs	High-temperature heat-treatment	/	0.77 V vs. RHE	[93]
NDCN	graphene/silica nanosheet	templating approach	589	-0.13 V vs. Ag/AgCl	[30]
N,S-hcs	carbon sphere	soft template approach	583	0.81 V vs. RHE	[96]
NSCNT-3	partially exfoliated MWCNTs	High-temperature heat-treatment	472.5	0.81 V vs. RHE	[99]
NDCNRs	PANI-PPy	carbonization	/	0.86 V vs. RHE	[106]

4. Conclusions and Outlooks

The low-cost, readily available, high electronic conductivity, and environmental friendly characteristics of carbon-based nanomaterials correspond to their great potential in renewable energy devices. After doping with N in the carbon frameworks, the electronic structure is changed, resulting in

excellent ORR performance, including superior ORR activity, long-term durability, and high methanol tolerance. These features have attracted tremendous attention to metal-free electrocatalyst for ORR to replace Pt/C. In this review, we summarized the synthesis strategy of N-doped nanomaterials, including the co-pyrolysis of carbon materials and N-containing sources, the pyrolysis of biomass materials, and direct pyrolysis of N-containing carbon-based materials. However, the catalytic activity of N-doped metal-free catalysts is still unsatisfactory for fuel cells and metal air batteries.

Great efforts have been devoted to further enhance the ORR performance, such as coordination with other heteroatoms (e.g., S and P), modification of carbon structure, and introduction of defects, which effectively improved the ORR performance on the basis of N-doped carbon materials. Through synergistic effects, the coordination of N with other heteroatoms can enhance the catalytic activity. The design of nanomaterials with various nanostructures and the coexistence of one-dimensional and two-dimensional structures can provide sufficient active sites for the catalytic process. The introduction of defects in the carbon base material can change the distribution of the electron density and electronic charge, which can benefit the ORR process. It should be noted that all the above strategies are not independent of each other. N doped into the carbon nanomaterials not only change the electron density and polarize the carbon matrix, but can also create defects in the carbon nanomaterials, which is generally ignored. Thus, the combination of each strategy is also an effective method to optimize the catalytic activity.

Apart from the above-mentioned strategies, there are still some potential methods to further enhance the catalytic performance. The tuning of the pore size distribution affects the catalytic performance. Mesopores exhibit quicker and more complete transport toward/from the catalytic sites for the reactants and products relative to micropores [108]. Using various strategies to enhance the specific surface area, such as an NaCl template [109] and carbon dioxide (CO₂) activation [72], can create abundant active sites for ORR. The content of N in the nanomaterials can affect the catalytic activity [110], although this method is still controversial.

The development of N-doped carbon-based nanomaterials in the future should focus on the design of specific structures with high specific surface area, abundant mesopores and macropores, optimal nitrogen content, rich defects, and so on. Besides, the development of test devices that accurately imitate real batteries to assess the capability of these new catalysts is becoming a new tendency in the field. Even though graphitic N or pyridinic N are more likely to act as the ORR active sites according to the above-mentioned research, more evidence is required, since the effect of the N bonding state on ORR activity is still under debate.

Author Contributions: Z.W. and J.W. conceived and wrote the review; M.S. searched the reported papers; X.L. checked the review overall.

Acknowledgments: This study was supported by Doctoral Found of QUST (010022873; 0100229001), Natural Science Foundation of Shandong Province of China (ZR2017MB054).

Conflicts of Interest: The authors declare no conflicts of interest.

References

1. Zhou, X.; Qiao, J.; Yang, L.; Zhang, J. A review of graphene-based nanostructural materials for both catalyst supports and metal-free catalysts in pem fuel cell oxygen reduction reactions. *Adv. Energy Mater.* **2014**, *4*, 1301523. [[CrossRef](#)]
2. Zheng, Y.; Jiao, Y.; Qiao, S.Z. Engineering of carbon-based electrocatalysts for emerging energy conversion: From fundamentality to functionality. *Adv. Mater.* **2015**, *27*, 5372–5378. [[CrossRef](#)] [[PubMed](#)]
3. Rivera, L.; Fajardo, S.; Arévalo, M.; García, G.; Pastor, E. S- and N-Doped graphene nanomaterials for the oxygen reduction reaction. *Catalysts* **2017**, *7*, 278.
4. Bu, L.; Ding, J.; Guo, S.; Zhang, X.; Su, D.; Zhu, X.; Yao, J.; Guo, J.; Lu, G.; Huang, X. A general method for multimetallic platinum alloy nanowires as highly active and stable oxygen reduction catalysts. *Adv. Mater.* **2015**, *27*, 7204–7212. [[CrossRef](#)] [[PubMed](#)]

5. Xia, W.; Li, J.; Wang, T.; Song, L.; Guo, H.; Gong, H.; Jiang, C.; Gao, B.; He, J. The synergistic effect of ceria and co in N-doped leaf-like carbon nanosheets derived from a 2D MOF and their enhanced performance in the oxygen reduction reaction. *Chem. Commun.* **2018**, *54*, 1623–1626. [[CrossRef](#)] [[PubMed](#)]
6. Sumboja, A.; Lübke, M.; Wang, Y.; An, T.; Zong, Y.; Liu, Z. All-solid-state, foldable, and rechargeable Zn-air batteries based on manganese oxide grown on graphene-coated carbon cloth air cathode. *Adv. Energy Mater.* **2017**, *7*, 1700927. [[CrossRef](#)]
7. Guan, C.; Sumboja, A.; Wu, H.; Ren, W.; Liu, X.; Zhang, H.; Liu, Z.; Cheng, C.; Pennycook, S.J.; Wang, J. Hollow Co₃O₄ nanosphere embedded in carbon arrays for stable and flexible solid-state zinc–air batteries. *Adv. Mater.* **2017**, *29*, 1704117. [[CrossRef](#)] [[PubMed](#)]
8. Tang, Z.; Pei, Z.; Wang, Z.; Li, H.; Zeng, J.; Ruan, Z.; Huang, Y.; Zhu, M.; Xue, Q.; Yu, J.; et al. Highly anisotropic, multichannel wood carbon with optimized heteroatom doping for supercapacitor and oxygen reduction reaction. *Carbon* **2018**, *130*, 532–543. [[CrossRef](#)]
9. Wang, D.; Liu, S.; Wang, J.; Lin, R.; Kawasaki, M.; Rus, E.; Silberstein, K.E.; Lowe, M.A.; Lin, F.; Nordlund, D.; et al. Spontaneous incorporation of gold in palladium-based ternary nanoparticles makes durable electrocatalysts for oxygen reduction reaction. *Nat. Commun.* **2016**, *7*, 11941. [[CrossRef](#)] [[PubMed](#)]
10. Sun, M.; Davenport, D.; Liu, H.; Qu, J.; Elimelech, M.; Li, J. Highly efficient and sustainable non-precious-metal Fe–N–C electrocatalysts for the oxygen reduction reaction. *J. Mater. Chem. A* **2018**, *6*, 2527–2539. [[CrossRef](#)]
11. Jin, X.; Xie, Y.; Huang, J. Highly effective dual transition metal macrocycle based electrocatalyst with macro-/mesoporous structures for oxygen reduction reaction. *Catalysts* **2017**, *7*, 201. [[CrossRef](#)]
12. Wang, J.; Wu, Z.; Han, L.; Xuan, C.; Zhu, J.; Xiao, W.; Wu, J.; Xin, H.L.; Wang, D. A general approach for the direct fabrication of metal oxide-based electrocatalysts for efficient bifunctional oxygen electrodes. *Sustain. Energy Fuels* **2017**, *1*, 823–831. [[CrossRef](#)]
13. An, T.; Ge, X.; Tham, N.N.; Sumboja, A.; Liu, Z.; Zong, Y. Facile one-pot synthesis of CoFe alloy nanoparticles decorated N-doped carbon for high-performance rechargeable Zinc–air battery stacks. *ACS Sustain. Chem. Eng.* **2018**. [[CrossRef](#)]
14. She, Y.; Lu, Z.; Ni, M.; Li, L.; Leung, M.K.H. Facile synthesis of nitrogen and sulfur codoped carbon from ionic liquid as metal-free catalyst for oxygen reduction reaction. *ACS Appl. Mater. Interfaces* **2015**, *7*, 7214–7221. [[CrossRef](#)] [[PubMed](#)]
15. Yang, W.; Yue, X.; Liu, X.; Zhai, J.; Jia, J. N-derived N, S Co-doped ordered mesoporous carbon for high-performance oxygen reduction. *Nanoscale* **2015**, *7*, 11956–11961. [[CrossRef](#)] [[PubMed](#)]
16. Ge, X.; Sumboja, A.; Wu, D.; An, T.; Li, B.; Goh, F.T.; Hor, T.A.; Zong, Y.; Liu, Z. Oxygen reduction in alkaline media: From mechanisms to recent advances of catalysts. *ACS Catal.* **2015**, *5*, 4643–4667. [[CrossRef](#)]
17. Cui, H.J.; Yu, H.M.; Zheng, J.F.; Wang, Z.J.; Zhu, Y.Y.; Jia, S.P.; Jia, J.; Zhu, Z.P. N-doped graphene frameworks with superhigh surface area: Excellent electrocatalytic performance for oxygen reduction. *Nanoscale* **2016**, *8*, 2795–2803. [[CrossRef](#)] [[PubMed](#)]
18. Jeon, I.-Y.; Zhang, S.; Zhang, L.; Choi, H.-J.; Seo, J.-M.; Xia, Z.; Dai, L.; Baek, J.-B. Edge-selectively sulfurized graphene nanoplatelets as efficient metal-free electrocatalysts for oxygen reduction reaction: The electron spin effect. *Adv. Mater.* **2013**, *25*, 6138–6145. [[CrossRef](#)] [[PubMed](#)]
19. Wu, J.; Jin, C.; Yang, Z.; Tian, J.; Yang, R. Synthesis of phosphorus-doped carbon hollow spheres as efficient metal-free electrocatalysts for oxygen reduction. *Carbon* **2015**, *82*, 562–571. [[CrossRef](#)]
20. Yang, L.; Jiang, S.; Zhao, Y.; Zhu, L.; Chen, S.; Wang, X.; Wu, Q.; Ma, J.; Ma, Y.; Hu, Z. Boron-doped carbon nanotubes as metal-free electrocatalysts for the oxygen reduction reaction. *Angew. Chem.* **2011**, *123*, 7270–7273. [[CrossRef](#)]
21. Baek, J.Y.; Jeon, I.-Y.; Baek, J.-B. Edge-iodine/sulfonic acid-functionalized graphene nanoplatelets as efficient electrocatalysts for oxygen reduction reaction. *J. Mater. Chem. A* **2014**, *2*, 8690–8695. [[CrossRef](#)]
22. Gong, K.; Du, F.; Xia, Z.; Durstock, M.; Dai, L. Nitrogen-doped carbon nanotube arrays with high electrocatalytic activity for oxygen reduction. *Science* **2009**, *323*, 760–764. [[CrossRef](#)] [[PubMed](#)]
23. Guo, D.; Shibuya, R.; Akiba, C.; Saji, S.; Kondo, T.; Nakamura, J. Active sites of nitrogen-doped carbon materials for oxygen reduction reaction clarified using model catalysts. *Science* **2016**, *351*, 361–365. [[CrossRef](#)] [[PubMed](#)]
24. Wu, Z.; Wang, J.; Han, L.; Lin, R.; Liu, H.; Xin, H.L.; Wang, D. Supramolecular gel-assisted synthesis of double shelled Co@CoO@N-C/C nanoparticles with synergistic electrocatalytic activity for the oxygen reduction reaction. *Nanoscale* **2016**, *8*, 4681–4687. [[CrossRef](#)] [[PubMed](#)]

25. Ding, W.; Li, L.; Xiong, K.; Wang, Y.; Li, W.; Nie, Y.; Chen, S.; Qi, X.; Wei, Z. Shape fixing via salt recrystallization: A morphology-controlled approach to convert nanostructured polymer to carbon nanomaterial as a highly active catalyst for oxygen reduction reaction. *J. Am. Chem. Soc.* **2015**, *137*, 5414–5420. [[CrossRef](#)] [[PubMed](#)]
26. Zhang, L.; Xia, Z. Mechanisms of oxygen reduction reaction on nitrogen-doped graphene for fuel cells. *J. Phys. Chem. C* **2011**, *115*, 11170–11176. [[CrossRef](#)]
27. Yang, H.B.; Miao, J.; Hung, S.-F.; Chen, J.; Tao, H.B.; Wang, X.; Zhang, L.; Chen, R.; Gao, J.; Chen, H.M.; et al. Identification of catalytic sites for oxygen reduction and oxygen evolution in N-doped graphene materials: Development of highly efficient metal-free bifunctional electrocatalyst. *Sci. Adv.* **2016**, *2*, e1501122. [[CrossRef](#)] [[PubMed](#)]
28. Wu, Z.; Song, M.; Wang, J. Supramolecular gel assisted synthesis of Co₂P nanosheets as efficient and stable catalyst for oxygen reduction reaction. *New J. Chem.* **2018**. [[CrossRef](#)]
29. Higgins, D.; Chen, Z.; Chen, Z. Nitrogen doped carbon nanotubes synthesized from aliphatic diamines for oxygen reduction reaction. *Electrochim. Acta* **2011**, *56*, 1570–1575. [[CrossRef](#)]
30. Wei, W.; Liang, H.; Parvez, K.; Zhuang, X.; Feng, X.; Müllen, K. Nitrogen-doped carbon nanosheets with size-defined mesopores as highly efficient metal-free catalyst for the oxygen reduction reaction. *Angew. Chem.* **2014**, *126*, 1596–1600. [[CrossRef](#)]
31. Tuci, G.; Zafferoni, C.; Rossin, A.; Milella, A.; Luconi, L.; Innocenti, M.; Truong Phuoc, L.; Duong-Viet, C.; Pham-Huu, C.; Giambastiani, G. Chemically functionalized carbon nanotubes with pyridine groups as easily tunable N-decorated nanomaterials for the oxygen reduction reaction in alkaline medium. *Chem. Mater.* **2014**, *26*, 3460–3470. [[CrossRef](#)]
32. Jin, Z.; Yao, J.; Kittrell, C.; Tour, J.M. Large-scale growth and characterizations of nitrogen-doped monolayer graphene sheets. *ACS Nano* **2011**, *5*, 4112–4117. [[CrossRef](#)] [[PubMed](#)]
33. Ma, F.-X.; Wang, J.; Wang, F.-B.; Xia, X.-H. The room temperature electrochemical synthesis of N-doped graphene and its electrocatalytic activity for oxygen reduction. *Chem. Commun.* **2015**, *51*, 1198–1201. [[CrossRef](#)] [[PubMed](#)]
34. Antolini, E. Graphene as a new carbon support for low-temperature fuel cell catalysts. *Appl. Catal. B Environ.* **2012**, *123–124*, 52–68. [[CrossRef](#)]
35. Ma, Y.; Sun, L.; Huang, W.; Zhang, L.; Zhao, J.; Fan, Q.; Huang, W. Three-dimensional nitrogen-doped carbon nanotubes/graphene structure used as a metal-free electrocatalyst for the oxygen reduction reaction. *J. Phys. Chem. C* **2011**, *115*, 24592–24597. [[CrossRef](#)]
36. Gao, S.; Liu, H.; Geng, K.; Wei, X. Honeysuckles-derived porous nitrogen, sulfur, dual-doped carbon as high-performance metal-free oxygen electroreduction catalyst. *Nano Energy* **2015**, *12*, 785–793. [[CrossRef](#)]
37. Wohlgemuth, S.-A.; White, R.J.; Willinger, M.-G.; Titirici, M.-M.; Antonietti, M. A one-pot hydrothermal synthesis of sulfur and nitrogen doped carbon aerogels with enhanced electrocatalytic activity in the oxygen reduction reaction. *Green Chem.* **2012**, *14*, 1515–1523. [[CrossRef](#)]
38. Shamsunnahar, S.M.; Nagai, M. Nitrogen doping of ash-free coal and effect of ash components on properties and oxygen reduction reaction in fuel cell. *Fuel* **2014**, *126*, 134–142. [[CrossRef](#)]
39. Choi, C.H.; Chung, M.W.; Park, S.H.; Woo, S.I. Additional doping of phosphorus and/or sulfur into nitrogen-doped carbon for efficient oxygen reduction reaction in acidic media. *Phys. Chem. Chem. Phys.* **2013**, *15*, 1802–1805. [[CrossRef](#)] [[PubMed](#)]
40. Qiao, X.; Liao, S.; You, C.; Chen, R. Phosphorus and nitrogen dual doped and simultaneously reduced graphene oxide with high surface area as efficient metal-free electrocatalyst for oxygen reduction. *Catalysts* **2015**, *5*, 981–991. [[CrossRef](#)]
41. Xue, Y.; Yu, D.; Dai, L.; Wang, R.; Li, D.; Roy, A.; Lu, F.; Chen, H.; Liu, Y.; Qu, J. Three-dimensional B,N-doped graphene foam as a metal-free catalyst for oxygen reduction reaction. *Phys. Chem. Chem. Phys.* **2013**, *15*, 12220–12226. [[CrossRef](#)] [[PubMed](#)]
42. Meng, K.; Liu, Q.; Huang, Y.; Wang, Y. Facile synthesis of nitrogen and fluorine Co-doped carbon materials as efficient electrocatalysts for oxygen reduction reactions in air-cathode microbial fuel cells. *J. Mater. Chem. A* **2015**, *3*, 6873–6877. [[CrossRef](#)]
43. Denis, P.A.; Huelmo, C.P.; Iribarne, F. Theoretical characterization of sulfur and nitrogen dual-doped graphene. *Comput. Theor. Chem.* **2014**, *1049*, 13–19. [[CrossRef](#)]

44. Ai, W.; Luo, Z.; Jiang, J.; Zhu, J.; Du, Z.; Fan, Z.; Xie, L.; Zhang, H.; Huang, W.; Yu, T. Nitrogen and sulfur Codoped graphene: Multifunctional electrode materials for high-performance Li-ion batteries and oxygen reduction reaction. *Adv. Mater.* **2014**, *26*, 6186–6192. [[CrossRef](#)] [[PubMed](#)]
45. Paraknowitsch, J.P.; Thomas, A. Doping carbons beyond nitrogen: An overview of advanced heteroatom doped carbons with boron, sulphur and phosphorus for energy applications. *Energy Environ. Sci.* **2013**, *6*, 2839–2855. [[CrossRef](#)]
46. Li, Y.; Li, L.; Zhu, L.; Gu, L.; Cao, X. Interlocked multi-armed carbon for stable oxygen reduction. *Chem. Commun.* **2016**, *52*, 5520–5522. [[CrossRef](#)] [[PubMed](#)]
47. Liang, J.; Zheng, Y.; Chen, J.; Liu, J.; Hulicova-Jurcakova, D.; Jaroniec, M.; Qiao, S.Z. Facile oxygen reduction on a three-dimensionally ordered macroporous graphitic C₃N₄/carbon composite electrocatalyst. *Angew. Chem.* **2012**, *124*, 3958–3962. [[CrossRef](#)]
48. Chen, L.; Du, R.; Zhu, J.; Mao, Y.; Xue, C.; Zhang, N.; Hou, Y.; Zhang, J.; Yi, T. Three-dimensional nitrogen-doped graphene nanoribbons aerogel as a highly efficient catalyst for the oxygen reduction reaction. *Small* **2015**, *11*, 1423–1429. [[CrossRef](#)] [[PubMed](#)]
49. Sidik, R.A.; Anderson, A.B.; Subramanian, N.P.; Kumaraguru, S.P.; Popov, B.N. O₂ reduction on graphite and nitrogen-doped graphite: Experiment and theory. *J. Phys. Chem. B* **2006**, *110*, 1787–1793. [[CrossRef](#)] [[PubMed](#)]
50. Tao, G.; Zhang, L.; Chen, L.; Cui, X.; Hua, Z.; Wang, M.; Wang, J.; Chen, Y.; Shi, J. N-doped hierarchically macro/mesoporous carbon with excellent electrocatalytic activity and durability for oxygen reduction reaction. *Carbon* **2015**, *86*, 108–117. [[CrossRef](#)]
51. Liu, Q.; Duan, Y.; Zhao, Q.; Pan, F.; Zhang, B.; Zhang, J. Direct synthesis of nitrogen-doped carbon nanosheets with high surface area and excellent oxygen reduction performance. *Langmuir* **2014**, *30*, 8238–8245. [[CrossRef](#)] [[PubMed](#)]
52. Li, Y.; Zhang, H.; Liu, P.; Wang, Y.; Yang, H.; Li, Y.; Zhao, H. Self-supported bimodal-pore structured nitrogen-doped carbon fiber aerogel as electrocatalyst for oxygen reduction reaction. *Electrochem. Commun.* **2015**, *51*, 6–10. [[CrossRef](#)]
53. Liu, F.; Peng, H.; You, C.; Fu, Z.; Huang, P.; Song, H.; Liao, S. High-performance doped carbon catalyst derived from nori biomass with melamine promoter. *Electrochim. Acta* **2014**, *138*, 353–359. [[CrossRef](#)]
54. Pan, F.; Cao, Z.; Zhao, Q.; Liang, H.; Zhang, J. Nitrogen-doped porous carbon nanosheets made from biomass as highly active electrocatalyst for oxygen reduction reaction. *J. Power Sources* **2014**, *272*, 8–15. [[CrossRef](#)]
55. Gao, S.; Chen, Y.; Fan, H.; Wei, X.; Hu, C.; Luo, H.; Qu, L. Large scale production of biomass-derived N-doped porous carbon spheres for oxygen reduction and supercapacitors. *J. Mater. Chem. A* **2014**, *2*, 3317–3324. [[CrossRef](#)]
56. Meng, Y.; Voiry, D.; Goswami, A.; Zou, X.; Huang, X.; Chhowalla, M.; Liu, Z.; Asefa, T. N-, O-, and S-tridoped nanoporous carbons as selective catalysts for oxygen reduction and alcohol oxidation reactions. *J. Am. Chem. Soc.* **2014**, *136*, 13554–13557. [[CrossRef](#)] [[PubMed](#)]
57. Gavrilov, N.; Pašti, I.A.; Mitrić, M.; Travas-Sejdić, J.; Ćirić-Marjanović, G.; Mentus, S.V. Electrocatalysis of oxygen reduction reaction on polyaniline-derived nitrogen-doped carbon nanoparticle surfaces in alkaline media. *J. Power Sources* **2012**, *220*, 306–316. [[CrossRef](#)]
58. Nam, G.; Park, J.; Kim, S.T.; Shin, D.-B.; Park, N.; Kim, Y.; Lee, J.-S.; Cho, J. Metal-free ketjenblack incorporated nitrogen-doped carbon sheets derived from gelatin as oxygen reduction catalysts. *Nano Lett.* **2014**, *14*, 1870–1876. [[CrossRef](#)] [[PubMed](#)]
59. Liu, X.; Li, L.; Zhou, W.; Zhou, Y.; Niu, W.; Chen, S. High-performance electrocatalysts for oxygen reduction based on nitrogen-doped porous carbon from hydrothermal treatment of glucose and dicyandiamide. *ChemElectroChem* **2015**, *2*, 803–810. [[CrossRef](#)]
60. Men, B.; Sun, Y.; Li, M.; Hu, C.; Zhang, M.; Wang, L.; Tang, Y.; Chen, Y.; Wan, P.; Pan, J. Hierarchical metal-free nitrogen-doped porous graphene/carbon composites as an efficient oxygen reduction reaction catalyst. *ACS Appl. Mater. Interfaces* **2016**, *8*, 1415–1423. [[CrossRef](#)] [[PubMed](#)]
61. Wang, Y.; Liu, H.; Wang, K.; Song, S.; Tsiakaras, P. 3D interconnected hierarchically porous N-doped carbon with NH₃ activation for efficient oxygen reduction reaction. *Appl. Catal. B Environ.* **2017**, *210*, 57–66. [[CrossRef](#)]
62. Wang, X.; Lee, J.S.; Zhu, Q.; Liu, J.; Wang, Y.; Dai, S. Ammonia-treated ordered mesoporous carbons as catalytic materials for oxygen reduction reaction. *Chem. Mater.* **2010**, *22*, 2178–2180. [[CrossRef](#)]

63. Zhou, T.; Zhou, Y.; Ma, R.; Zhou, Z.; Liu, G.; Liu, Q.; Zhu, Y.; Wang, J. Nitrogen-doped hollow mesoporous carbon spheres as a highly active and stable metal-free electrocatalyst for oxygen reduction. *Carbon* **2017**, *114*, 177–186. [[CrossRef](#)]
64. Li, X.; Fang, Y.; Zhao, S.; Wu, J.; Li, F.; Tian, M.; Long, X.; Jin, J.; Ma, J. Nitrogen-doped mesoporous carbon nanosheet/carbon nanotube hybrids as metal-free bi-functional electrocatalysts for water oxidation and oxygen reduction. *J. Mater. Chem. A* **2016**, *4*, 13133–13141. [[CrossRef](#)]
65. Pan, F.; Jin, J.; Fu, X.; Liu, Q.; Zhang, J. Advanced oxygen reduction electrocatalyst based on nitrogen-doped graphene derived from edible sugar and urea. *ACS Appl. Mater. Interfaces* **2013**, *5*, 11108–11114. [[CrossRef](#)] [[PubMed](#)]
66. Liu, Z.; Zhang, G.; Lu, Z.; Jin, X.; Chang, Z.; Sun, X. One-step scalable preparation of N-doped nanoporous carbon as a high-performance electrocatalyst for the oxygen reduction reaction. *Nano Res.* **2013**, *6*, 293–301. [[CrossRef](#)]
67. Li, J.-C.; Hou, P.-X.; Zhao, S.-Y.; Liu, C.; Tang, D.-M.; Cheng, M.; Zhang, F.; Cheng, H.-M. A 3D bi-functional porous N-doped carbon microtube sponge electrocatalyst for oxygen reduction and oxygen evolution reactions. *Energy Environ. Sci.* **2016**, *9*, 3079–3084. [[CrossRef](#)]
68. Liang, H.-W.; Wu, Z.-Y.; Chen, L.-F.; Li, C.; Yu, S.-H. Bacterial cellulose derived nitrogen-doped carbon nanofiber aerogel: An efficient metal-free oxygen reduction electrocatalyst for zinc-air battery. *Nano Energy* **2015**, *11*, 366–376. [[CrossRef](#)]
69. Chen, P.; Wang, L.-K.; Wang, G.; Gao, M.-R.; Ge, J.; Yuan, W.-J.; Shen, Y.-H.; Xie, A.-J.; Yu, S.-H. Nitrogen-doped nanoporous carbon nanosheets derived from plant biomass: An efficient catalyst for oxygen reduction reaction. *Energy Environ. Sci.* **2014**, *7*, 4095–4103. [[CrossRef](#)]
70. Graglia, M.; Pampel, J.; Hantke, T.; Fellingner, T.-P.; Esposito, D. Nitro lignin-derived nitrogen-doped carbon as an efficient and sustainable electrocatalyst for oxygen reduction. *ACS Nano* **2016**, *10*, 4364–4371. [[CrossRef](#)] [[PubMed](#)]
71. Zhao, J.; Liu, Y.; Quan, X.; Chen, S.; Yu, H.; Zhao, H. Nitrogen-doped carbon with a high degree of graphitization derived from biomass as high-performance electrocatalyst for oxygen reduction reaction. *Appl. Surf. Sci.* **2017**, *396*, 986–993. [[CrossRef](#)]
72. Sui, Z.-Y.; Li, X.; Sun, Z.-Y.; Tao, H.-C.; Zhang, P.-Y.; Zhao, L.; Han, B.-H. Nitrogen-doped and nanostructured carbons with high surface area for enhanced oxygen reduction reaction. *Carbon* **2018**, *126*, 111–118. [[CrossRef](#)]
73. Deng, H.; Li, Q.; Liu, J.; Wang, F. Active sites for oxygen reduction reaction on nitrogen-doped carbon nanotubes derived from polyaniline. *Carbon* **2017**, *112*, 219–229. [[CrossRef](#)]
74. Zhang, L.; Su, Z.; Jiang, F.; Yang, L.; Qian, J.; Zhou, Y.; Li, W.; Hong, M. Highly graphitized nitrogen-doped porous carbon nanopolyhedra derived from ZIF-8 nanocrystals as efficient electrocatalysts for oxygen reduction reactions. *Nanoscale* **2014**, *6*, 6590–6602. [[CrossRef](#)] [[PubMed](#)]
75. Zhao, X.; Zhao, H.; Zhang, T.; Yan, X.; Yuan, Y.; Zhang, H.; Zhao, H.; Zhang, D.; Zhu, G.; Yao, X. One-step synthesis of nitrogen-doped microporous carbon materials as metal-free electrocatalysts for oxygen reduction reaction. *J. Mater. Chem. A* **2014**, *2*, 11666–11671. [[CrossRef](#)]
76. Yang, L.; Zeng, X.; Wang, W.; Cao, D. Recent progress in MOF-derived, heteroatom-doped porous carbons as highly efficient electrocatalysts for oxygen reduction reaction in fuel cells. *Adv. Funct. Mater.* **2018**, *28*, 1704537. [[CrossRef](#)]
77. Xiang, Z.; Mercado, R.; Huck, J.M.; Wang, H.; Guo, Z.; Wang, W.; Cao, D.; Haranczyk, M.; Smit, B. Systematic tuning and multifunctionalization of covalent organic polymers for enhanced carbon capture. *J. Am. Chem. Soc.* **2015**, *137*, 13301–13307. [[CrossRef](#)] [[PubMed](#)]
78. Usov, P.M.; McDonnell-Worth, C.; Zhou, F.; MacFarlane, D.R.; D'Alessandro, D.M. The electrochemical transformation of the zeolitic imidazolate framework ZIF-67 in aqueous electrolytes. *Electrochim. Acta* **2015**, *153*, 433–438. [[CrossRef](#)]
79. Wang, J.-H.; Li, M.; Li, D. A dynamic, luminescent and entangled mof as a qualitative sensor for volatile organic solvents and a quantitative monitor for acetonitrile vapour. *Chem. Sci.* **2013**, *4*, 1793–1801. [[CrossRef](#)]
80. Li, L.; Dai, P.; Gu, X.; Wang, Y.; Yan, L.; Zhao, X. High oxygen reduction activity on a metal-organic framework derived carbon combined with high degree of graphitization and pyridinic-N dopants. *J. Mater. Chem. A* **2017**, *5*, 789–795. [[CrossRef](#)]
81. Jiang, M.; Cao, X.; Zhu, D.; Duan, Y.; Zhang, J. Hierarchically porous N-doped carbon derived from ZIF-8 nanocomposites for electrochemical applications. *Electrochim. Acta* **2016**, *196*, 699–707. [[CrossRef](#)]

82. Qu, K.; Zheng, Y.; Dai, S.; Qiao, S.Z. Graphene oxide-polydopamine derived N, S-codoped carbon nanosheets as superior bifunctional electrocatalysts for oxygen reduction and evolution. *Nano Energy* **2016**, *19*, 373–381. [[CrossRef](#)]
83. Zhao, G.; Shi, L.; Xu, J.; Yan, X.; Zhao, T.S. Role of phosphorus in nitrogen, phosphorus dual-doped ordered mesoporous carbon electrocatalyst for oxygen reduction reaction in alkaline media. *Int. J. Hydrog. Energy* **2018**, *43*, 1470–1478. [[CrossRef](#)]
84. Borghei, M.; Laocharoen, N.; Kibena-Pöldsepp, E.; Johansson, L.-S.; Campbell, J.; Kauppinen, E.; Tammeveski, K.; Rojas, O.J. Porous N,P-doped carbon from coconut shells with high electrocatalytic activity for oxygen reduction: Alternative to Pt-C for alkaline fuel cells. *Appl. Catal. B Environ.* **2017**, *204*, 394–402. [[CrossRef](#)]
85. Jiang, H.; Wang, Y.; Hao, J.; Liu, Y.; Li, W.; Li, J. N and P Co-functionalized three-dimensional porous carbon networks as efficient metal-free electrocatalysts for oxygen reduction reaction. *Carbon* **2017**, *122*, 64–73. [[CrossRef](#)]
86. Yang, J.; Sun, H.; Liang, H.; Ji, H.; Song, L.; Gao, C.; Xu, H. A highly efficient metal-free oxygen reduction electrocatalyst assembled from carbon nanotubes and graphene. *Adv. Mater.* **2016**, *28*, 4606–4613. [[CrossRef](#)] [[PubMed](#)]
87. Geim, A.K.; Novoselov, K.S. The rise of graphene. *Nat. Mater.* **2007**, *6*, 183–191. [[CrossRef](#)] [[PubMed](#)]
88. Novoselov, K.S. Cracking bilayers. *Nat. Phys.* **2009**, *5*, 862–863. [[CrossRef](#)]
89. Lee, C.; Wei, X.; Kysar, J.W.; Hone, J. Measurement of the elastic properties and intrinsic strength of monolayer graphene. *Science* **2008**, *321*, 385–388. [[CrossRef](#)] [[PubMed](#)]
90. Wan, K.; Tan, A.-D.; Yu, Z.-P.; Liang, Z.-X.; Piao, J.-H.; Tsiakaras, P. 2D nitrogen-doped hierarchically porous carbon: Key role of low dimensional structure in favoring electrocatalysis and mass transfer for oxygen reduction reaction. *Appl. Catal. B Environ.* **2017**, *209*, 447–454. [[CrossRef](#)]
91. Zhang, J.; Zhang, M.; Lin, L.; Wang, X. Sol processing of conjugated carbon nitride powders for thin-film fabrication. *Angew. Chem.* **2015**, *127*, 6395–6399. [[CrossRef](#)]
92. Li, Q.; Xu, D.; Ou, X.; Yan, F. Nitrogen-doped graphitic porous carbon nanosheets derived from in situ formed g-C₃N₄ templates for the oxygen reduction reaction. *Chem. Asian J.* **2017**, *12*, 1816–1823. [[CrossRef](#)] [[PubMed](#)]
93. Yu, H.; Shang, L.; Bian, T.; Shi, R.; Waterhouse, G.I.N.; Zhao, Y.; Zhou, C.; Wu, L.-Z.; Tung, C.-H.; Zhang, T. Nitrogen-Doped Porous Carbon Nanosheets Templated from g-C₃N₄ as Metal-Free Electrocatalysts for Efficient Oxygen Reduction Reaction. *Adv. Mater.* **2016**, *28*, 5080–5086. [[CrossRef](#)] [[PubMed](#)]
94. Chai, G.S.; Shin, I.S.; Yu, J.S. Synthesis of ordered, uniform, macroporous carbons with mesoporous walls templated by aggregates of polystyrene spheres and silica particles for use as catalyst supports in direct methanol fuel cells. *Adv. Mater.* **2004**, *16*, 2057–2061. [[CrossRef](#)]
95. Wu, M.; Wang, J.; Wu, Z.; Xin, H.L.; Wang, D. Synergistic enhancement of nitrogen and sulfur Co-doped graphene with carbon nanosphere insertion for the electrocatalytic oxygen reduction reaction. *J. Mater. Chem. A* **2015**, *3*, 7727–7731. [[CrossRef](#)]
96. Wu, Z.; Liu, R.; Wang, J.; Zhu, J.; Xiao, W.; Xuan, C.; Lei, W.; Wang, D. Nitrogen and sulfur Co-doping of 3D hollow-structured carbon spheres as an efficient and stable metal free catalyst for the oxygen reduction reaction. *Nanoscale* **2016**, *8*, 19086–19092. [[CrossRef](#)] [[PubMed](#)]
97. Wang, J.; Wu, Z.; Han, L.; Lin, R.; Xin, H.L.; Wang, D. Hollow-structured carbon-supported nickel cobaltite nanoparticles as an efficient bifunctional electrocatalyst for the oxygen reduction and evolution reactions. *ChemCatChem* **2016**, *8*, 736–742. [[CrossRef](#)]
98. Wang, J.; Xin, H.L.; Zhu, J.; Liu, S.; Wu, Z.; Wang, D. 3D hollow structured Co₂FeO₄/MWCNT as an efficient non-precious metal electrocatalyst for oxygen reduction reaction. *J. Mater. Chem. A* **2015**, *3*, 1601–1608. [[CrossRef](#)]
99. Wang, J.; Wu, Z.; Han, L.; Lin, R.; Xiao, W.; Xuan, C.; Xin, H.L.; Wang, D. Nitrogen and sulfur Co-doping of partially exfoliated MWCNTs as 3-D structured electrocatalysts for the oxygen reduction reaction. *J. Mater. Chem. A* **2016**, *4*, 5678–5684. [[CrossRef](#)]
100. Xia, B.; Yan, Y.; Wang, X.; Lou, X.W. Recent progress on graphene-based hybrid electrocatalysts. *Mater. Horiz.* **2014**, *1*, 379–399. [[CrossRef](#)]
101. Yang, S.; Zhi, L.; Tang, K.; Feng, X.; Maier, J.; Müllen, K. Efficient synthesis of heteroatom (N or S)-doped graphene based on ultrathin graphene oxide-porous silica sheets for oxygen reduction reactions. *Adv. Funct. Mater.* **2012**, *22*, 3634–3640. [[CrossRef](#)]

102. Jiang, Y.; Yang, L.; Sun, T.; Zhao, J.; Lyu, Z.; Zhuo, O.; Wang, X.; Wu, Q.; Ma, J.; Hu, Z. Significant contribution of intrinsic carbon defects to oxygen reduction activity. *ACS Catal.* **2015**, *5*, 6707–6712. [[CrossRef](#)]
103. Zhao, X.; Zou, X.; Yan, X.; Brown, C.L.; Chen, Z.; Zhu, G.; Yao, X. Defect-driven oxygen reduction reaction (ORR) of carbon without any element doping. *Inorg. Chem. Front.* **2016**, *3*, 417–421. [[CrossRef](#)]
104. Zhao, H.; Sun, C.; Jin, Z.; Wang, D.-W.; Yan, X.; Chen, Z.; Zhu, G.; Yao, X. Carbon for the oxygen reduction reaction: A defect mechanism. *J. Mater. Chem. A* **2015**, *3*, 11736–11739. [[CrossRef](#)]
105. Yan, D.; Li, Y.; Huo, J.; Chen, R.; Dai, L.; Wang, S. Defect chemistry of nonprecious-metal electrocatalysts for oxygen reactions. *Adv. Mater.* **2017**, *29*, 1606459. [[CrossRef](#)] [[PubMed](#)]
106. He, J.; He, Y.; Fan, Y.; Zhang, B.; Du, Y.; Wang, J.; Xu, P. Conjugated polymer-mediated synthesis of nitrogen-doped carbon nanoribbons for oxygen reduction reaction. *Carbon* **2017**, *124*, 630–636. [[CrossRef](#)]
107. Oh, H.-S.; Oh, J.-G.; Lee, W.H.; Kim, H.-J.; Kim, H. The influence of the structural properties of carbon on the oxygen reduction reaction of nitrogen modified carbon based catalysts. *Int. J. Hydrog. Energy* **2011**, *36*, 8181–8186. [[CrossRef](#)]
108. Ferrero, G.A.; Preuss, K.; Fuertes, A.B.; Sevilla, M.; Titirici, M.M. The influence of pore size distribution on the oxygen reduction reaction performance in nitrogen doped carbon microspheres. *J. Mater. Chem. A* **2016**, *4*, 2581–2589. [[CrossRef](#)]
109. Zheng, X.; Cao, X.; Li, X.; Tian, J.; Jin, C.; Yang, R. Biomass lysine-derived nitrogen-doped carbon hollow cubes via a nacl crystal template: An efficient bifunctional electrocatalyst for oxygen reduction and evolution reactions. *Nanoscale* **2017**, *9*, 1059–1067. [[CrossRef](#)] [[PubMed](#)]
110. Chatterjee, K.; Ashokkumar, M.; Gullapalli, H.; Gong, Y.; Vajtai, R.; Thanikaivelan, P.; Ajayan, P.M. Nitrogen-rich carbon nano-onions for oxygen reduction reaction. *Carbon* **2018**, *130*, 645–651. [[CrossRef](#)]



© 2018 by the authors. Licensee MDPI, Basel, Switzerland. This article is an open access article distributed under the terms and conditions of the Creative Commons Attribution (CC BY) license (<http://creativecommons.org/licenses/by/4.0/>).